Journal of Structural Geology, Vol. 8, Nos. 8, pp. 857 to 870, 1986
Printed in Great Britain

0191-8141/86 $03.00 + 0.00
Pergamon Journals Ltd.

Dynamic recrystallization and fabric development during the simple shear deformation of ice*

J. P. BURG, C. J. L. WILSON and J. C. MITCHELL

School of Earth Sciences, University of Melbourne, Parkville, Victoria 3052, Australia

(*Received* 19 *September* 1985; *accepted in revised form* 20 *January* 1986)

Abstract—*In situ* observations of polycrystalline ice deformed in simple shear between −10 and −1°C are presented. This study illustrates the processes responsible for the deformation, the development of a preferred crystallographic orientation and the formation of a preferred dimensional orientation. Intracrystalline glide on the basal plane, accompanying grain rotations and dynamic recrystallization, helps to accommodate the large intragranular strains. These are the most important mechanisms for crystallographic reorientation and produce a stable fabric that favours glide on the basal plane. Localized kinks, developed in grains unfavourably oriented for easy glide, are unstable and are overprinted by dynamic recrystallization. Dynamic recrystallization is a strain softening process with nucleation occurring in the form of equiaxed grains that grow subparallel to pre-existing grain anisotropies and become elongate during deformation. Plots of grain axial ratio against orientation ($R/\bar{\phi}$) indicate a weak shape fabric which does not correspond to the theoretical foliation and elongation for the appropriate increment of shear strain. We argue that estimates of the strain magnitude made from orientation of elongate grains are unreliable in high temperature shear zones. These results are applicable to both geological and glacial shear environments.

INTRODUCTION

SHEAR strain localization is the manifestation of an instability in plastic deformation of polycrystalline materials, the plastic flow concentrating along the directions characteristic of the slip-line field as soon as the material approximates the ideal plastic state (Chakrabarti & Spretnak 1975, Poirier 1980, Hutchinson & Tvergaard 1981). Shear zones are thus narrow domains on the maximum resolved shear-stress plane due to plastic yielding of the material in compression or extension (Rudnicki & Rice 1975, Poirier 1976, Jonas *et al.* 1976, Mandl *et al.* 1977). Across the ductile shear zones, markers are displaced and in the ideal geometry of simple shear there is no component of shortening or elongation orthogonal to the shear zone boundaries. Within the shear zone all the points are displaced in a direction parallel to the shear zone boundaries. Such displacements can only be attributed to deformation by simple shear to allow for compatibility of the strains in the shear zone (e.g. Ramsay & Graham 1970, Coward 1976, Cobbold 1977 for natural examples in rocks).

Narrow shear zones of intense laminar flow are movement zones with fundamental tectonic significance because they can lead to important kinematic interpretations (e.g. Escher *et al.* 1975, Nicolas *et al.* 1977, Burg *et al.* 1981, Davis 1983). One of the fundamental problems in such zones is to relate the strain state to the degree of deformation and determine the mechanical conditions which produce failure by plastic yielding (see discussions in White *et al.* 1980). To answer some of these questions an experimental approach with geometrically controlled conditions is of paramount importance.

The aim of this paper is to illustrate the mechanisms of deformation and development of a preferred crystallographic orientation and foliation during the simple shear of a grain aggregate. We have used polycrystalline ice as an analogue of easily deformed quartz-rich rocks (Wilson 1979), as it has been shown that there is a similarity between individual shear-zones in ice and those developed in massive crystalline rocks (Hudleston 1980). Ice is an ideal mineral analogue because of its hexagonal crystal structure and anisotropic slip activity on (0001). We believe that the results obtained are relevant to all environments involving polycrystalline aggregates deformed at high temperatures. They are applicable to both geological and glacial environments.

EXPERIMENTAL PROCEDURE

Observations on the development of inhomogeneous shear strain and the preferred crystallographic orientations of ice have been experimentally made in compression by Kamb (1972) and in torsion to simulate simple shear by Kamb (1972), Duval (1981) and Bouchez & Duval (1982). The apparatus (Fig. 1) used in this investigation permits the in-situ recording of the changes in an ice layer during progressive simple shear. A rectangular section of ice 25 × 35 mm and 0.85 mm thick has its lower and upper surfaces confined between two fixed glass plates (Fig. 1a). The two long edges are constrained to remain parallel by a fixed guide along one, and a sliding plate along the other (Fig. 1b); the travel of the latter is also constrained by a fixed guide. Shear stress is applied laterally to one end by a row of ten moveable

* A video movie illustrating aspects of shear deformation and recrystallization described in this paper may be purchased by writing to C. J. L. Wilson.

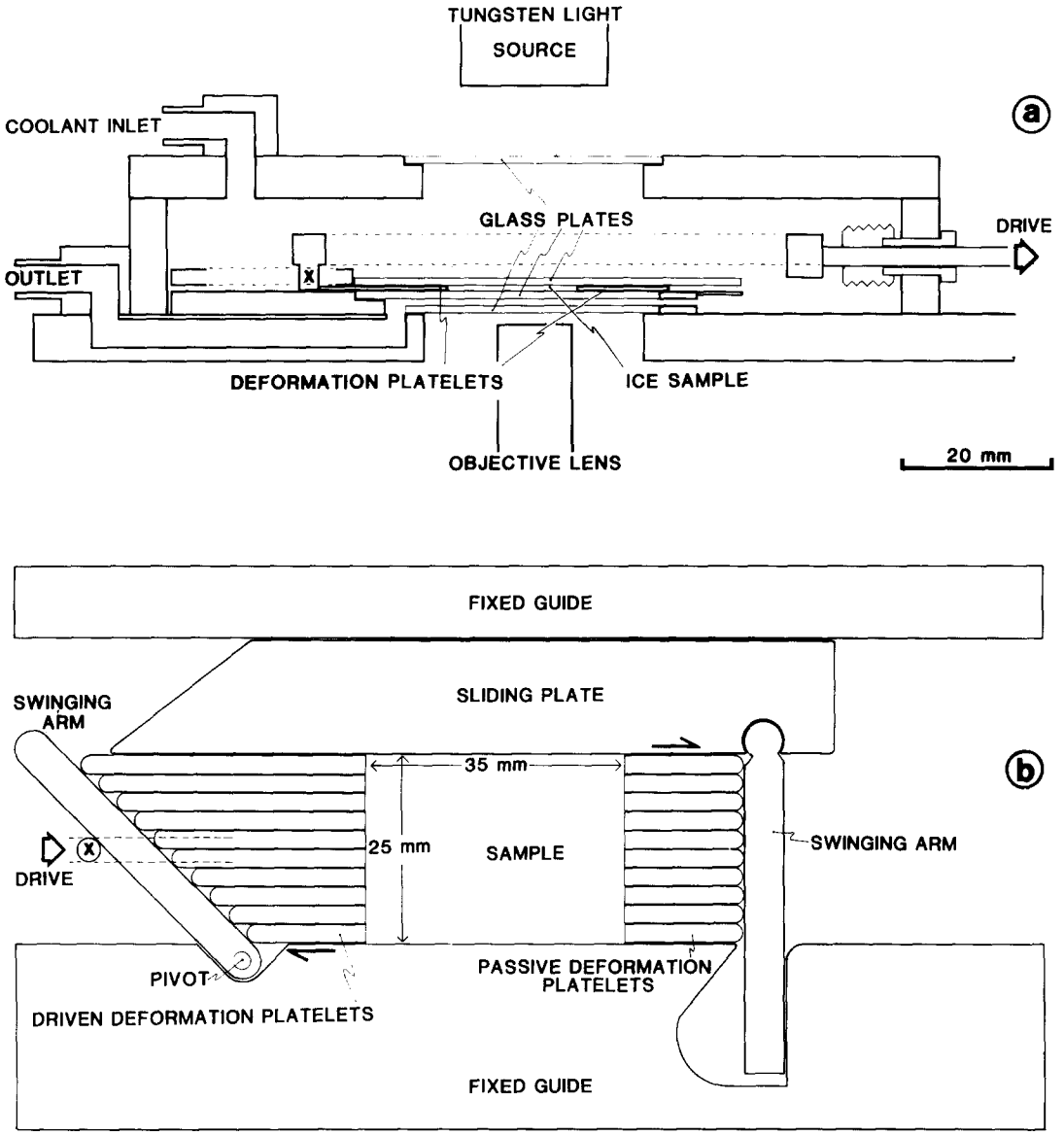

Fig. 1. In-situ simple shear deformation apparatus. (a) Section showing location of sample with respect to box containing coolant and the microscope objective lens and light source. (b) Plan view of the apparatus at the start of an experiment. At the pivot X the drive moves the swinging arm in a dextral sense.

platelets pushed by a swinging arm which pivots at one end so as to sweep an arc of ~50° (Fig. 1b). This arm is driven by a motor which acts through a gearbox and a micrometer. A similar set of platelets at the other end ensures a bulk simple shear of the ice with shear-strain γ ranging up to ~1. The final shape approximates a parallelogram with a step development in the two ends being due to angular terminations of the sliding platelets. While the drive operates at a constant speed and the load is applied parallel to the shear direction, there is a variation in the shear rate $\dot{\gamma}$ because of the circular type motion of the swinging arm to which the load is applied (Fig. 2). This shear rate variation is shown in Fig. 3. The apparatus is enclosed by a sealed box (Fig. 1a) through which refrigerated silicone oil is pumped to produce a temperature stability of ±0.2°C. The box is then mounted on a Zeiss Invertoscope and microstructural data are recorded from selected areas and between crossed polarized light, using a time-lapse system, on 16 mm and 35 mm film every 5 min and 5 h, respectively.

The laboratory-made ice used in this investigation was prepared by refreezing a mixture of sieved crushed ice and distilled water [see technical description in Wilson & Russell-Head (1982)]. The samples initially consisted of

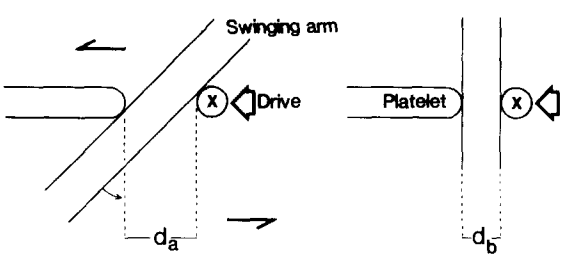

Fig. 2. Details of the load transfer from the drive to the platelets showing the effective decrease in width (d_a-d_b) of the swinging arm as it rotates about the pivot point X.

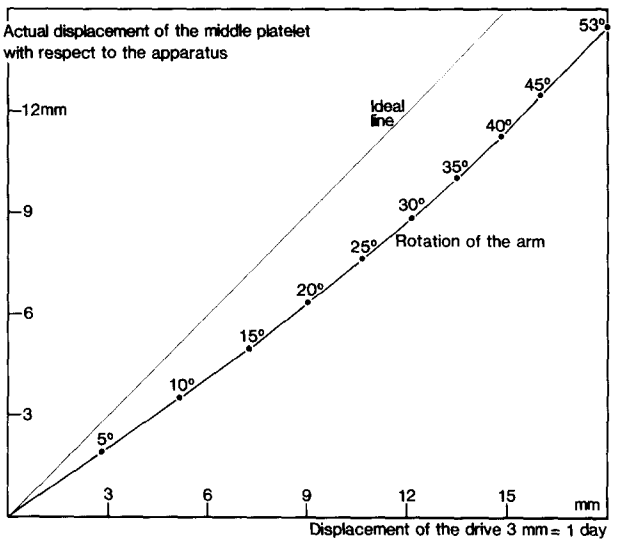

Fig. 3. The rate of angular shear change with a constant displacement of the drive.

equant and randomly oriented polygonal grains (mean grain size 2–5 mm) with small (0.1–0.2 mm) spherical air bubbles. The 'artificial' ice was therefore statistically isotropic and measurements showed that it did not display a preferred crystallographic orientation (Fig. 4).

Temperatures, durations and the final shear strain γ of the eight experiments described in this paper are presented in Table 1. In all experiments the imposed drive rate governing the amount of shear was 3 mm per day (Fig. 3). In order to test the heterogeneity of strain due to the apparatus, one experiment (SS10) involved the deformation of a single crystal whose glide-plane was oriented sub-parallel to the ice-layer plane. At an intermediate stage and with the completion of each experiment the whole sample was photographed. At the end of an experiment samples were unloaded and stored at temperatures below −14°C, in order to prevent microstructural readjustments of the deformed aggregate, prior to undertaking *c*-axis fabric measurements on a Rigsby Stage (Langway 1958).

RESULTS

Strain homogeneity

The thin layers of polycrystalline ice deformed homogeneously on the sample scale with little boundary effects adjacent to the sliding platelets. Heterogeneities at the boundary due to the small steps associated with the platelets produced a non-uniform deformation that penetrated no more than two grain diameters (i.e. <2 mm into the deformed sample. In all polycrystalline samples there was no detectable increase in thickness of the ice-layer during deformation so that the deformation was essentially plane-strain. For SS10, however, the orientation of the single crystal was incompatible with slip on the basal plane. This resulted in the development of kinks (Fig. 5) and a ~25% extension in the direction

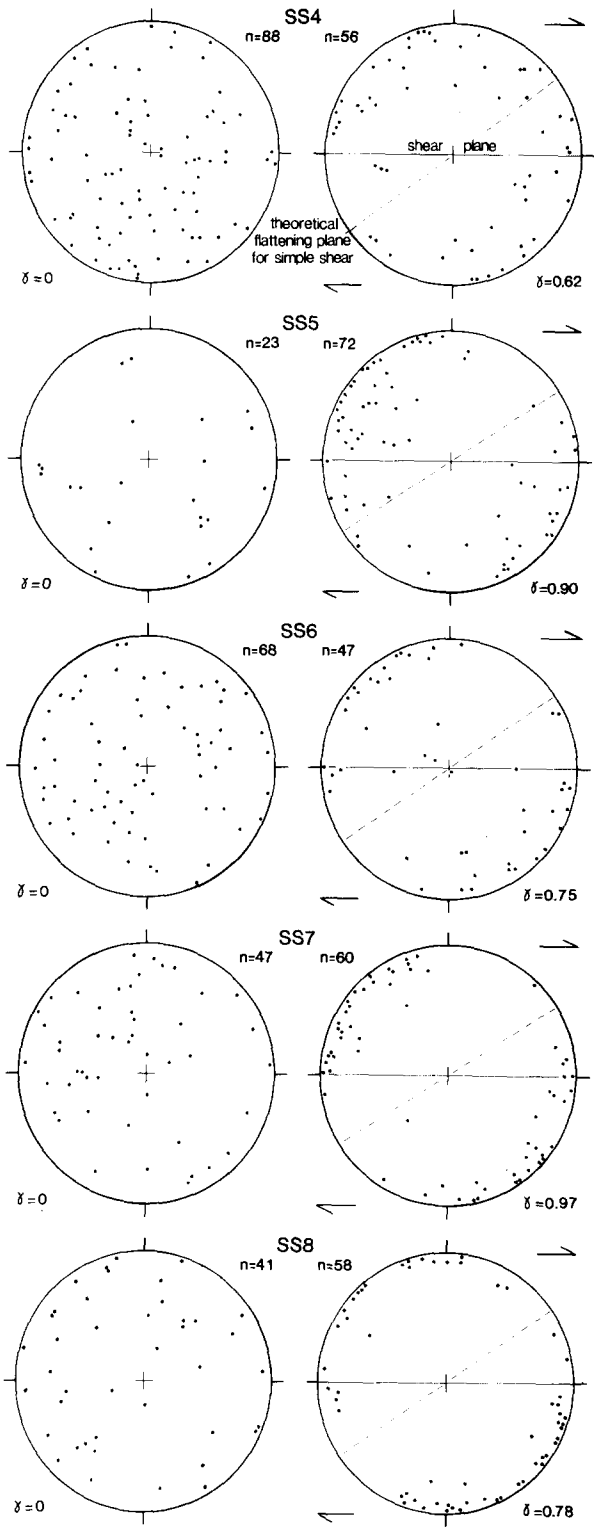

Fig. 4. Patterns of ice *c*-axes. Fabrics of the undeformed sample are on the left, and the fabrics produced as a result of dextral shear at different values of shear strain (γ) are on the right. *n*, number of measurements.

perpendicular to the ice layer produced through a redistribution of the silicon oil film adjacent to the ice layer. In this case the deformation departed noticeably from simple shear, a result attributed to the peculiar orientation conditions which were imposed for this experiment. The two ends of the deformed sample SS4 were not parallel (~15° to each other). This deviation from the expected geometry is also attributed to the effect of

Table 1. Summary of the simple-shear deformation experiments. In experiment SS10 the low shear strain can be attributed to a thickening of the sample

Experiment number	Experiment duration (days and hours)	Temperature (°C)	Final shear strain (γ)	Average size ($\bar{A}$ = mm² × magnification) and axial ratio $\bar{R}$ at different stages during deformation		
				Initial	Intermediate	Final
SS3	3–23	−4	0.45	$\bar{A}$ 948	485	689
				$\bar{R}$ 1.74	2.06	1.91
SS4	4–00	−4	0.62	$\bar{A}$ —	—	609
				$\bar{R}$ —	—	2.43
SS5	7–18	−5	0.9	$\bar{A}$ 1218	—	508
				$\bar{R}$ 2.04	—	2.3
SS6	5–20	−5	0.75	$\bar{A}$ 1315	—	612
				$\bar{R}$ 1.94	—	2.07
SS7	7–19	−1.3	0.97	$\bar{A}$ —		440
				$\bar{R}$ —		2.17
SS8	6–03	−1	0.78	$\bar{A}$ 1428	786	740
				$\bar{R}$ 1.84	2.12	2.01
SS10	5–21	−10	0.45	—	—	—
SS11	5–14	−10	0.70	$\bar{A}$ 1399	—	450
				$\bar{R}$ 1.8	—	2.06

kinked grains oriented with their gliding planes at high angles to the shear plane.

The spatial distribution of air bubbles or clusters of air bubbles could be used as markers of displacement and hence local deformation relative to a chosen point (e.g. points A–D in Fig. 6). Inter-grain strain trajectories recognized in the deformed state are generally indicative of consistent displacements subparallel to the constraining guides and with γ equal to the bulk shear strain for the whole sample. However, there are local heterogeneities in both orientation and magnitude of strain. These can be attributed to grains of different orientations which deformed and rotated at different rates, particularly those preserved as 'augen' (grain B in Fig. 6) in regions undergoing new grain nucleation and extensive grain shape changes.

Initially spherical air bubbles could not be used as classical finite strain markers. Their final elongation is strongly dependent on the initial orientation of the ice crystal, and the finite stretching direction of the bubbles depends on the amount of slip which has occurred within one individual grain. Grains favourably oriented for glide display very elongated air bubbles, while grains in which little basal slip has occurred still carry subspherical air bubbles. Therefore in the *in-situ* experiments the bubble orientations could not be used as a quantitative indicator of shear strain as they have for natural examples (Russell-Head & Budd 1979, Hudleston 1980). In areas undergoing recrystallization air bubbles are seldom preserved, except where they are an intra-grain feature preserved in augen or attached to a grain boundary of a relict grain. The air bubbles are expelled into the silicon oil because the sample is thin and the bubbles are near the surface.

Microstructures

All simple-shear experiments (except SS10) showed a comparable microstructural evolution (Fig. 6) over the whole range of temperature conditions investigated (Table 1). The first change is the development of sutured grain boundaries (Fig. 7). This occurs by migration of the original grain boundaries contemporaneous with the development of slip bands parallel to (0001) (Figs. 7a,b & f) but before there is any obvious change in *c*-axis orientation between neighbouring grains (less than 2°). This feature was attributed by Wilson (1986) to slip lamellae in adjacent grains interacting along a common grain boundary and is particularly obvious in grains that are oriented with the slip plane lying at an oblique angle to the surface of the sample.

Glide in suitably oriented grains is the dominant intracrystalline deformation mechanism. Glide within individual crystals is not uniform as suggested by the formation of undulose extinction and the subsequent development of deformation bands and kinks (grain B, Figs. 7c–e) which develop as an additional deformation mechanism (Wilson *et al.* 1986). While glide is restricted to the single slip system {0001}, grain boundary migration and rotation of neighbouring grains occur so that the grains fit together.

Nucleation of small new equiaxed grains (Figs. 6 and 7) appears at very small values of shear strain ($\gamma \leq 0.2$) with an obvious dependence on temperature; nucleation tends to start earlier for experiments SS7 and SS8 at −1°C than for the others. The distribution of recrystallization nuclei is irregular and the equiaxed shapes of the recrystallized grains are preserved as long as new grain boundary migration is unimportant. If migrating boundaries are pinned, the equiaxed shape was rapidly destroyed, with the development of a serrated interlocking grain structure.

At higher shear strains ($\gamma \leq 0.4$) the microstructures were qualitatively the same. They consisted of coarse undulose grains with well-developed slip bands (Fig. 6c), and serrated and embayed grain boundaries. Deformation bands and kinks were particularly well developed in grains unsuitably oriented for easy glide and consequently retained as deformed relicts or augen (grains B and E, Figs. 7b–e) oblique to the shear plane.

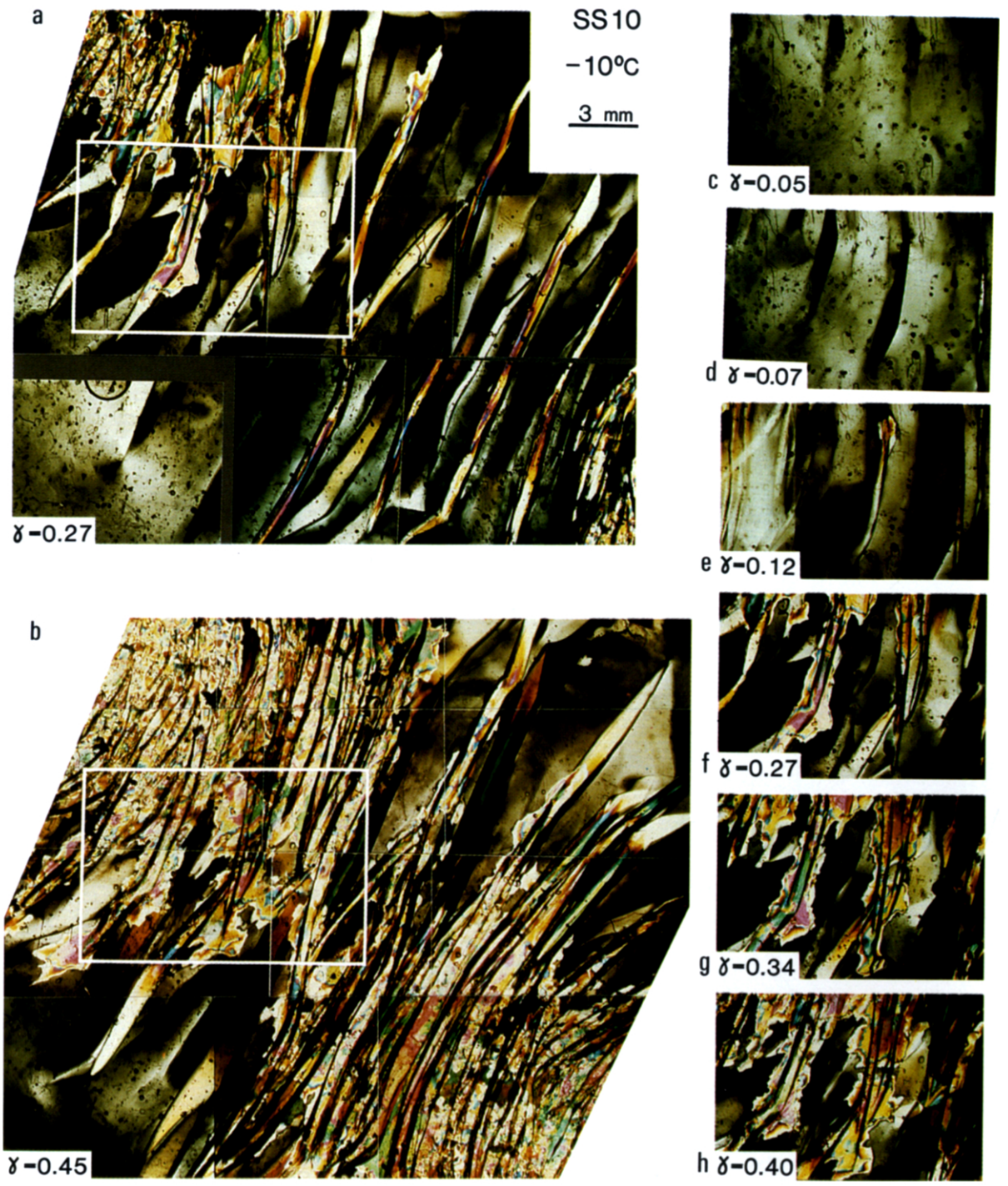

Fig. 5. Dextral deformation of single crystal with the basal plane subparallel to the plane of the ice layer. The outlined areas in (a) and (b) correspond to the region illustrated in the deformaton sequence (c–h).

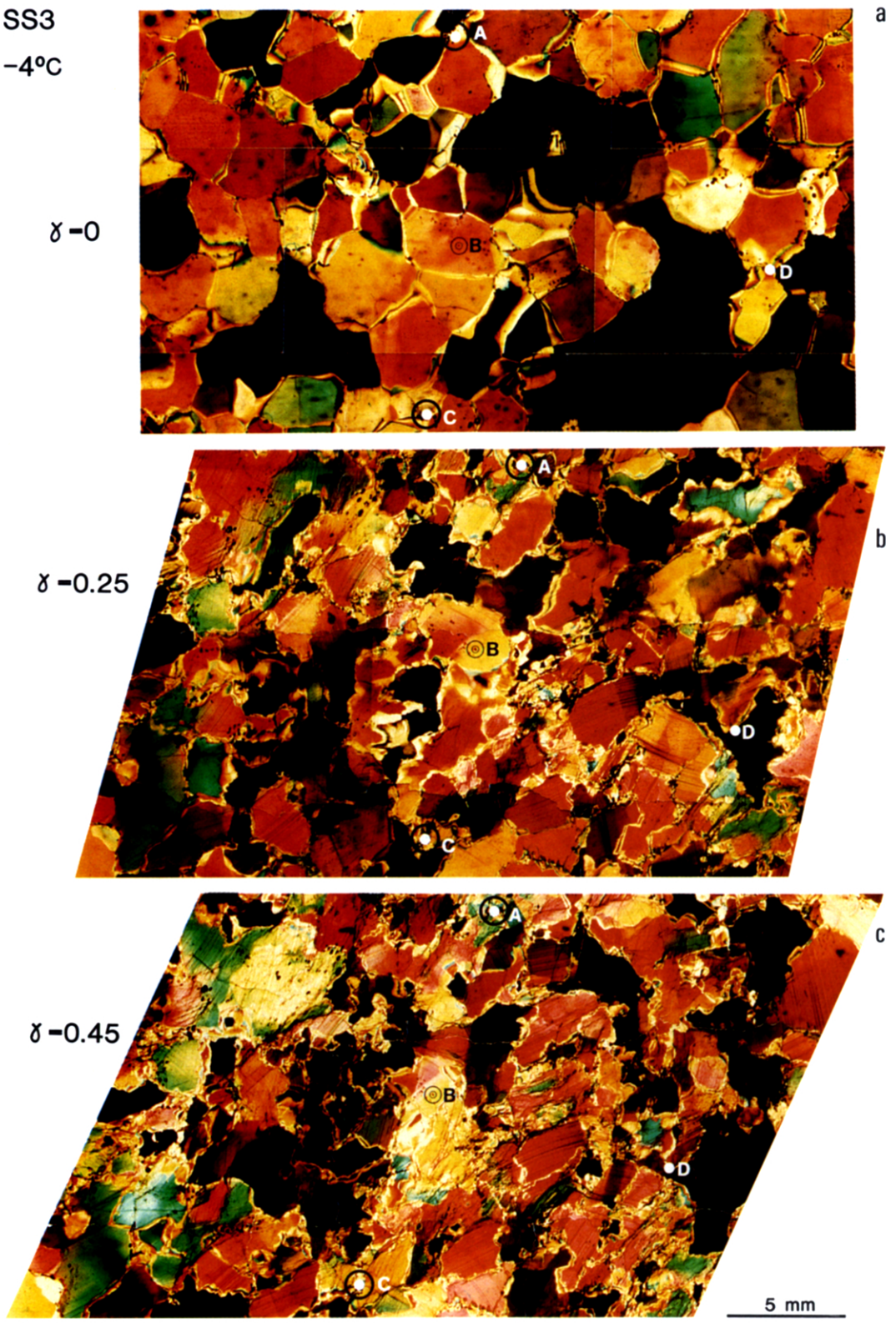

Fig. 6. Sample SS3 showing initial, intermediate and final stages of dextral simple shear at −4°C. The circled points A–D are positions of some air bubbles that were used as marker points in the sample. Note that the intra-grain air bubble B occurs within a grain that becomes kinked.

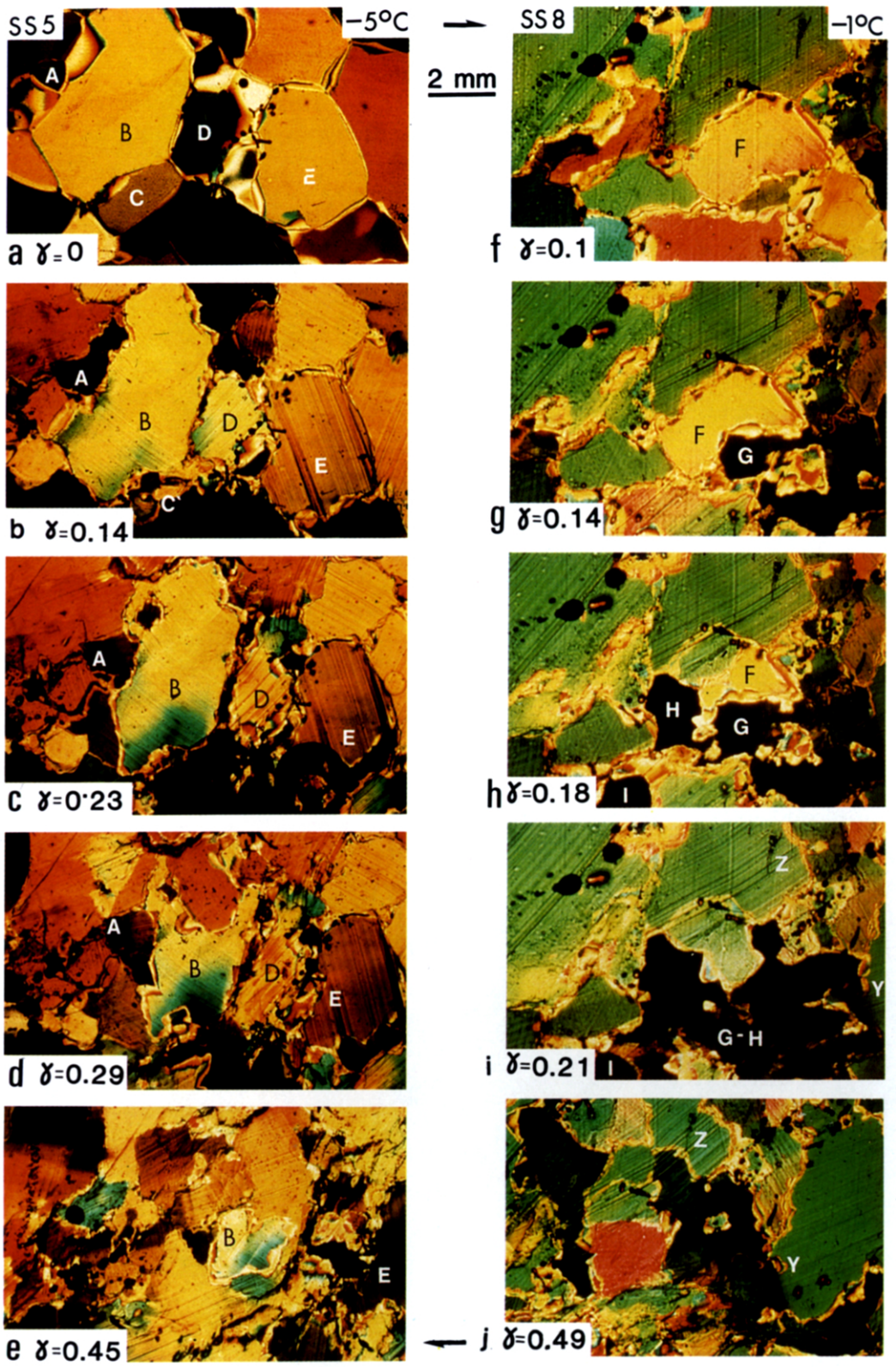

Fig. 7. Deformation sequence during the dextral shear of SS5 at −4°C (a–e) and SS8 at −1°C (f–j). In sequence (a–e). Grain A grows parallel to the direction of elongation, (b) is deformed and separated into three separate grains (c), with one subgrain (d) consuming part of grain B (e). Grain B is progressively reduced in size after initial grain-boundary adjustments and the development of slip bands. The slip bands are bent (c–d) and eventually become kinked (e). Grain C has been transformed by stage (b) into a group of subgrains with one subgrain C′ (b) growing and consuming the others (c). Grain D changes orientation (stage b) begins to form subgrains in (d) and disappears in (e) as a region of new grains that form a distinct zone that parallels the elongation direction. Grain E changes orientation but is preserved as an augen. In sequence (f–j). Adjacent to the weakly deformed grain F (stage f) equiaxed grains G, H and I (stages g & h) are nucleated. Grains G–H (stages h & i) undergo boundary migration and combine. Grains G, H and I undergo further shear with the formation of a new aggregate (stage j) sandwiched between and overgrowing deformed relict grains X and Y (i & j).

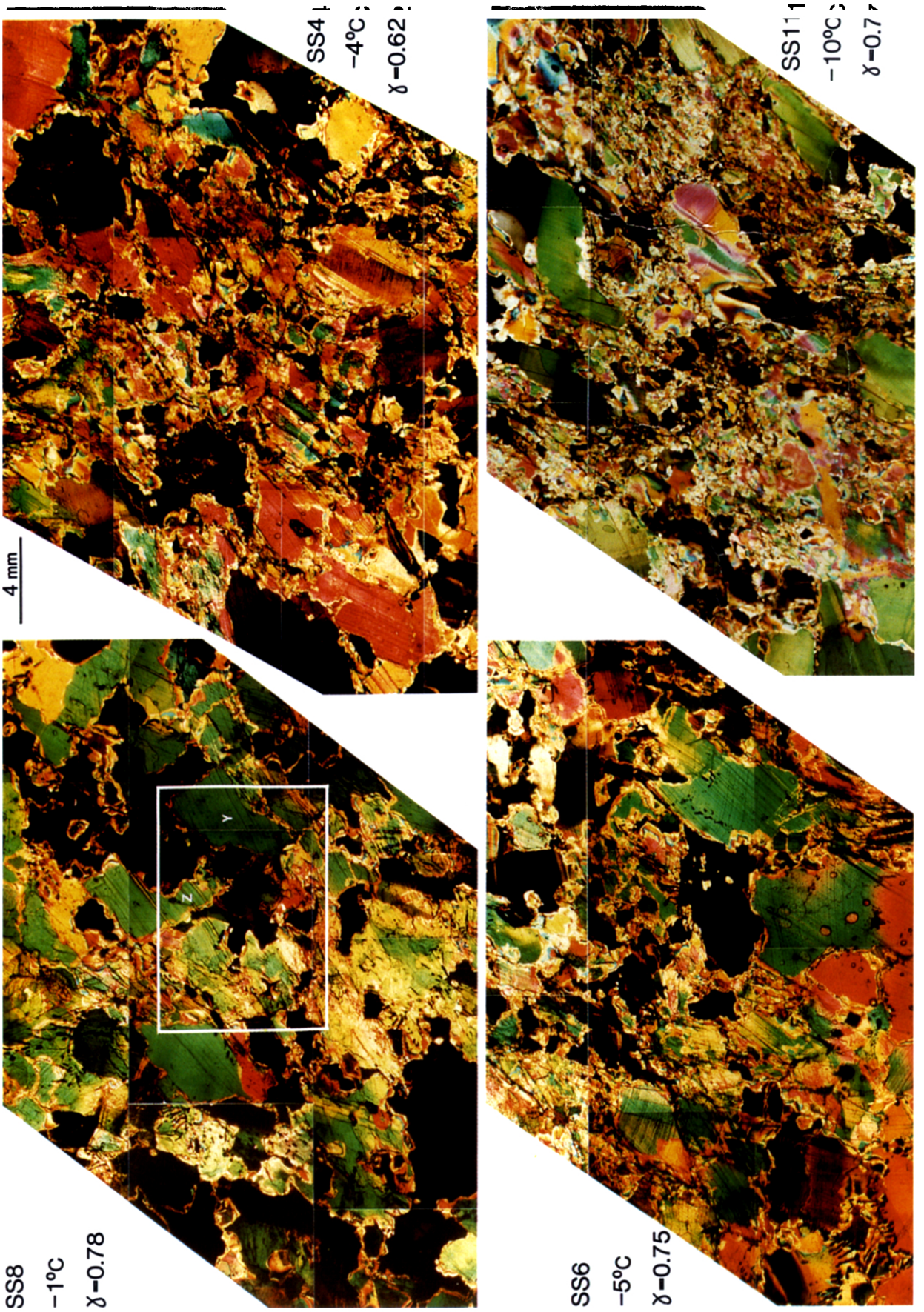

Fig. 8. The microstructure of the samples at the time of unloading of experiments SS8, SS4, SS6 and SS11. The outlined area in SS8 corresponds to the region illustrated in Fig. 7(j), but at a higher shear strain.

Between these are smaller irregular and equidimensional grains that preserve few or no deformation features. These equidimensional grains appear to be a product of dynamic recrystallization involving new grain nucleation at selective sites or of the breakdown of pre-existing grains in a hard-glide orientation (e.g. grain C in Fig. 7a which becomes a series of subgrains in Fig. 7b) through a mechanism of subgrain rotation as described by Wilson (1986). The transition from an equidimensional shape to an irregular shape suggests that the newly nucleated grains are undergoing large components of migration recrystallization (e.g. grain G, Figs. 7g–i) while also experiencing high intra-grain strains as they rapidly change orientation, develop slip bands, become undulose and eventually break down into new grains (e.g. grains C and D, SS5, Fig. 7). At temperatures lower than −4°C it is noticeable that these processes are confined to sites occupied by discrete old host-grains, with the new grain size being smaller than the original grain diameter. In the higher temperature experiments (≃1°C) nucleation of equiaxed grains was followed by rapid and extensive grain-boundary migration (SS8, Figs. 7f–i), independent grains coalescing to form larger grains (G–H in Figs. 7h & i). Sites which had been swept by a moving boundary were then preferential sites for subsequent grain nucleation (Fig. 7j) and further grain growth (see area that corresponds to Fig. 7j in SS8, Fig. 8).

At higher shear strains ($\gamma > 0.5$) the areas of selective grain refinement in all temperature regimes studied eventually become zones that are oriented oblique to the direction of shear. These are recognized by an alignment of augen and a zonal distribution of the new recrystallized grains which correspond to a deformation induced 'foliation' (Fig. 8).

In the single crystal experiment (SS10, Fig. 5) strain is localized as a pronounced non-homogeneous deformation occurring in the form of kink bands. The kink bands were progressively developed at a high angle (80–85°) to the shear direction in an 'en echelon' pattern (Figs. 5a & b). This pattern defines a domain which occupies about half of the specimen area along one of the ice layer diagonals. Further deformation is restricted to this domain. The sequence of photographs (Figs. 5c–h) shows the increasing deformation from a strain at which kink bands were first detected ($\gamma \sim 0.05$) up to a shear strain $\gamma \sim 0.4$ with the unloading of the specimen. The nucleation of kink bands at a high angle to the shear direction (close to the direction of no finite extension) gives rise to a rapid lengthwise propagation and rotation across the kink band boundary, followed by a period of relatively passive behaviour and no kink propagation. Rotation and bending of the first formed segments of the kink bands results in the development of a sigmoidal shape of individual kink bands (Figs. 5a & b). Bulk strains accumulated during the passive behaviour probably lead to sudden nucleation and growth of new and short kink bands oblique to the first ones (Fig. 5f). The obliquity between old and new kink bands indicates a clockwise rotation of the kinking direction, consistent with the dextral vorticity of the imposed deformation. Where rotation across the kink band is locked, as a result of its curvature, the kink band becomes a site for new grain nucleation. Elongate relicts of the single crystal, easily identifiable by their crystallographic orientation, contribute to a general grain elongation between the new recrystallized grains.

Orientation and grain size variation

The average orientation $\bar{\phi}$ of the grain long axes with respect to the shear plane (Fig. 9) and the average size $\bar{A}$ of the polycrystalline ice grains, using the long axis × short axis product as an area (A) determination, have been measured from photomicrograph mosaics covering a complete sample. The arithmetical mean $\bar{A}$ is sufficient to document the two-dimensional grain-size variations during the simple-shear experiments (Fig. 10).

During the first increments of the deformation there is an obvious grain size reduction (Figs. 9 and 10 and Table 1). This is associated with an increase in the number of grains and can be related to the formation of subgrains (e.g. grain C, Figs. 7a & b). Contemporaneous and post-dating this is grain boundary migration which leads to grain growth balanced by recrystallization processes. This is responsible for an apparently stable $\bar{A}$ value produced during further deformation (Table 1 and Figs. 9 and 10). It is also noticeable that the recrystallized grain size at −10°C is smaller than that developed in the higher temperature samples. This confirms the observations of other workers (e.g. Kuon & Jonas 1973, Jacka 1984) that the temperature is a fundamental parameter controlling the final grain size in ice, whereas the magnitude of the shear strain governs the distribution of a particular recrystallized grain size versus augen within a sample.

The intimate association of intracrystalline deformation with subgrain rotation, nucleation and grain growth is responsible for the rapid grain size reductions. There was little modification in the spatial distribution patterns between original grains. This can be demonstrated (e.g. Figs. 6 and 8) where the spatial distribution of individual augen, despite a translation in the direction of shear, remains reasonably constant. However, $\bar{\phi}$ does not correspond to the theoretical flattening plane for simple shear that should be at ~34 and ~39° where $\bar{\phi} = 26$ and 23° for SS8 and SS3, respectively (see Fig. 9). This discrepancy can be attributed to the effect of grain-boundary migration at high temperature, as the experiments have been conducted close to the melting point, rather than to a pre-deformation fabric (Lisle 1977).

In the grain aggregate, deforming by steady-state flow, a given grain flattens during progressive deformation and represents a foliation-forming element. Recrystallization and nucleation during the deformation produce strain-free grains which are not foliation-forming elements until they are deformed (Means 1981). Nucleation and grain growth as described above are clearly foliation-destroying processes. Our measurements were

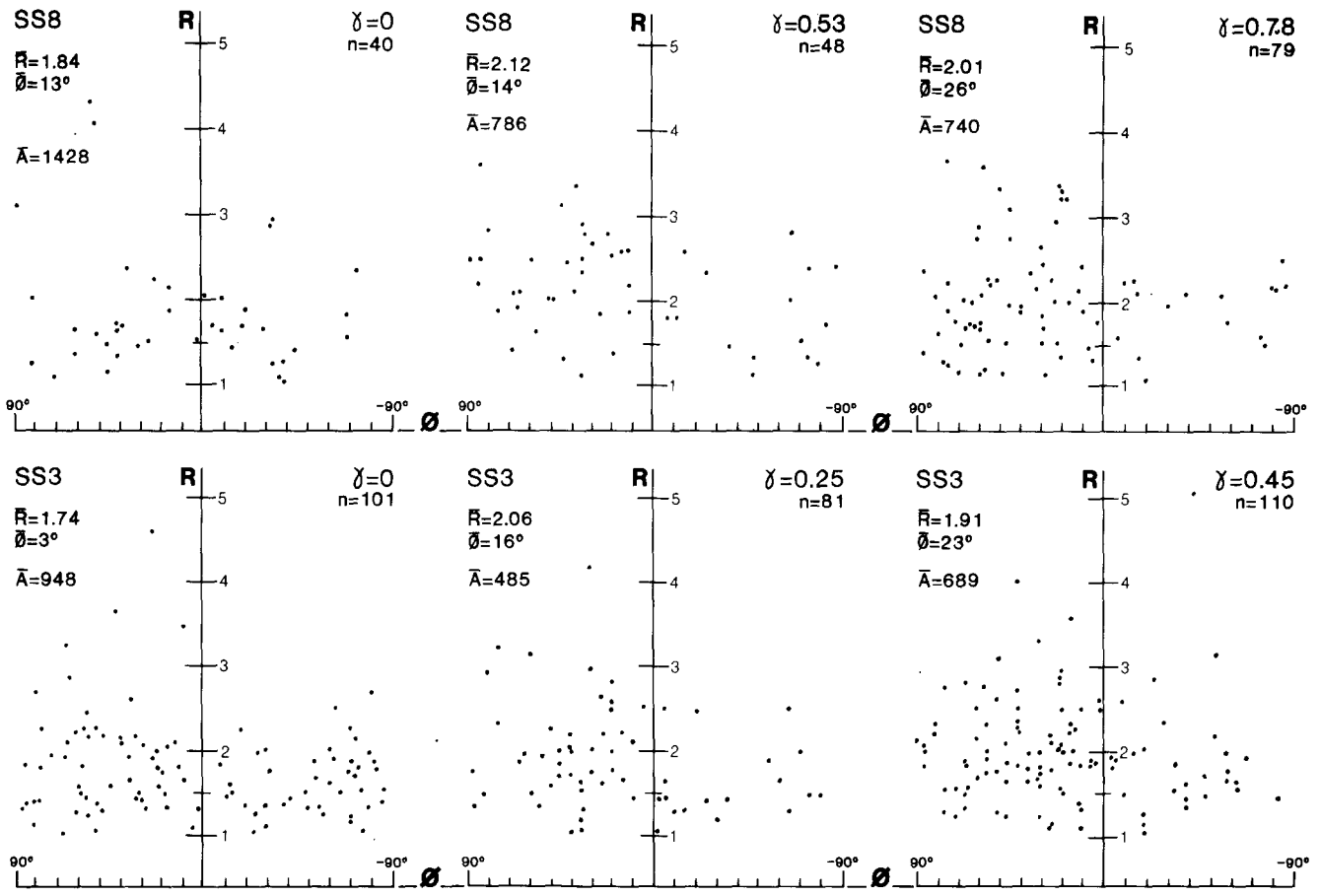

Fig. 9. The orientation (ϕ) and shape (axial ratio R) of ice grains in experiments SS8 and SS3, before, at an intermediate, and at the final stage of deformation. $\bar{R}$, average shape factor; $\bar{\phi}$, average orientation; γ, shear strain; $\bar{A}$, average size (mm^2 × magnification) and n, number of measurements.

from every grain in the section, including therefore relict grains which have undergone the total history and new recrystallized equiaxied grains which have suffered little shear deformation. Recrystallization and nucleation processes are responsible for the relatively stable measured shape and orientation fabric through the deformation (Fig. 9).

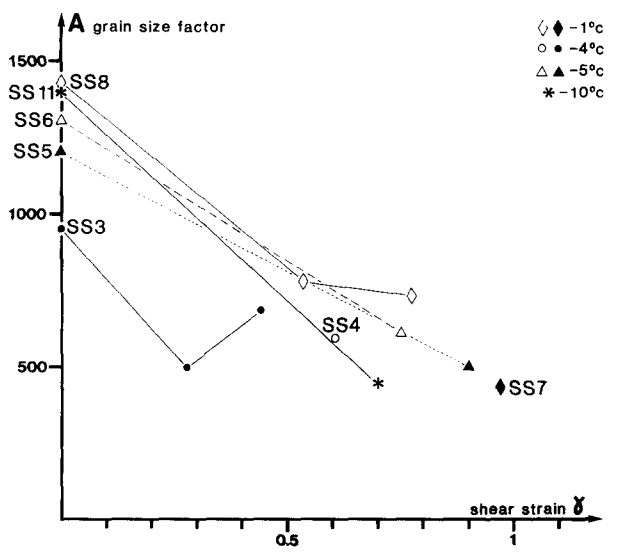

Fig. 10. Two dimensional grain size (mm^2 × magnification) variation with shear strain during the simple-shear deformation of polycrystalline ice.

c-axis orientations

c-axes of grains in both undeformed and deformed sections for each experiment were measured, when grain size made it possible. The most marked textural change is in the degree of preferred *c*-axis orientation, with increase from a random fabric to a pattern developing a strong single maximum oblique to the direction of flow (Fig. 4). This is particularly well illustrated by SS7 and SS8 (Fig. 4). The centres of the diagrams are devoid of any points whereas almost all the *c*-axes cluster along the borders of the NW and SE quadrants of the diagram for dextral shear. This pattern probably includes the two submaxima observed experimentally for equivalent shear strains of ice masses for both simple shear (Kamb 1972) and torsion (Kamb 1972, Bouchez & Duval 1982). The peripheral position on the diagram of most *c*-axes indicates that grains with an orientation of hard glide (i.e. basal plane close to the plane of the ice layer as for SS10) are eliminated during deformation. Syntectonic recrystallization and grain-boundary migration, attested by serrate grain boundaries along with the lack of a clearly marked foliation, may be the major accommodating processes. These processes give rise to a population of grains whose basal planes are at a high angle to the ice-layer plane and oblique to the shear plane. The shear strain reached with our experiments ($\gamma \leqslant 1$) is not large enough for the glide planes to have rotated towards

parallelism with the actual shear plane. The *c*-axis fabrics observed here are however consistent with the *c*-axis fabrics measured in natural and experimental shear deformation of ice, (Kamb 1972, Hudleston 1980, Bouchez & Duval 1982) and comparable with simulated patterns of crystallographic fabrics for aggregates that have undergone simple shear when one glide plane is dominant (Etchecopar 1977, Lister & Price 1978).

DISCUSSION

Dynamic recrystallization

A conspicuously active process in these simple-shear experiments, carried out at elevated temperatures (above half the melting point), is dynamic recrystallization. The first increments of deformation produce serrated boundaries due to grain-boundary migration and readjustments between neighbouring grains. This accompanies activation of slip on (0001), associated with new grain nucleation and grain growth.

The recrystallization processes are comparable to those described by Wilson (1986) for pure shear deformation of ice under similar physical conditions and appear to be dominated by migration of existing and new grain boundaries. They involve the break-up and rotation of old grains into subgrains, with subgrain development particularly noticeable in grains unsuitably oriented for easy glide. In addition, new equiaxed grains also appear to nucleate at grain boundary margins. The exact nucleation mechanism is unclear, but appears similar to the situation described by Ohtomo & Wakahama (1982). Migration of boundaries would evolve through dynamic processes, described as migration recrystallization by Poirier & Guillope (1979). However, there was little evidence of a bulge nucleation mechanism in these simple-shear experiments, although it has been described for pure shear in ice with a strong crystallographic orientation by Wilson (1986).

With each increment of deformation, recrystallization processes continuously modify individual grains or selective grain aggregates. Once a grain undergoes recrystallization, there will be a grain-size reduction prior to grain growth. The grain growth operates through coalescence or a boundary migration. As grain populations are continuously changing in number, size and shape, in regions undergoing recrystallization, it is not possible to correlate many of the recrystallized grains at particular strain increments except for the highly deformed relict grains or augen that may be preserved from the undeformed state. The areas of recrystallization are localised zones of ductile deformation and hence do not produce completely strain-free grains, whereas the augens represent 'hard spots'.

Foliation development

After shear strains of 10% a stable shape fabric is acquired. This is recognized by a relatively distinct recrystallized grain size distribution for a particular temperature regime. At lower temperatures and small shear strains it is marked by the presence of two grain populations, recrystallized grains vs augen. At higher temperatures or at larger shear strains the distinction between the two grain types is less obvious. Grain axial ratio plotted against orientation (R/ϕ) indicates a weak shape fabric (Fig. 9) which defines a preferred dimensional orientation that is not detectable by eye. The development of the preferred orientation can be considered as a combination of two mechanisms: (1) glide and rotation and (2) dynamic recrystallization.

Grain rotations occur with the onset of the intracrystalline deformation, namely the development of slip bands, and are associated with obvious birefringence changes that correspond to crystallographic changes (Fig. 4). As in the geometrical simulation of simple shear by Etchecopar (1977) two orientation regimes (Fig. 11a) govern the sense of grain rotation.

(1) Grains with basal planes oriented for easy glide (domains 1, Fig. 11a) generally rotate towards the direction of shear (Fig. 11b) with grains becoming highly elongate (e.g. grains Y in SS8, Fig. 8). Deformation of grains in domain 1a rarely produce the orientation and shape predicted in Etchecopar's model. Instead they rotate and continue to deform with (0001) parallel to the shear plane as a grain in domain 1b, but with a clockwise rotation. Unlike Etchecopar's model which involves homogeneous deformation on a grain scale, at higher strains the intracrystalline deformation becomes inhomogeneous developing undulose extinction (Fig. 11b) and intragranular shear localization. The latter is particularly obvious where the grain was initially elongated parallel to the basal plane and in extreme cases may produce ribbon-shaped grains as reported by Wilson *et al.* (1986). The importance of the grain rotations that produce the dimensional preferred orientation is to allow easier glide parallel to the shear plane direction.

(2) Grains oriented with (0001) at a high angle to the direction of shear (domain 2, Fig. 11a) undergo markedly irregular rotations (e.g. grain B, Fig. 7). After initial slip on the basal plane and rotation the grain is bent to produce either subgrains, deformation bands or kinks (Fig. 11b). Further strain is then accommodated by rotation between subgrains or across a deformation band or kink band boundary. Regions of extreme lattice rotation such as kink band boundaries (Fig. 5) then become sites for preferential grain growth and contribute to the reduction of grain size, leaving the old grain as an elongate relict or augen. These contribute to defining a shape fabric.

The preferred dimensional orientation probably owes its existence less to the preservation of elongate augen, as depicted in Fig. 11, than to the development of the dynamically recrystallized grains along preferential alignment directions. Where grains are undergoing grain growth they commonly do so by replacing or overgrowing existing grains such that the crystallographic orientation of some of the earlier grain population is pre-

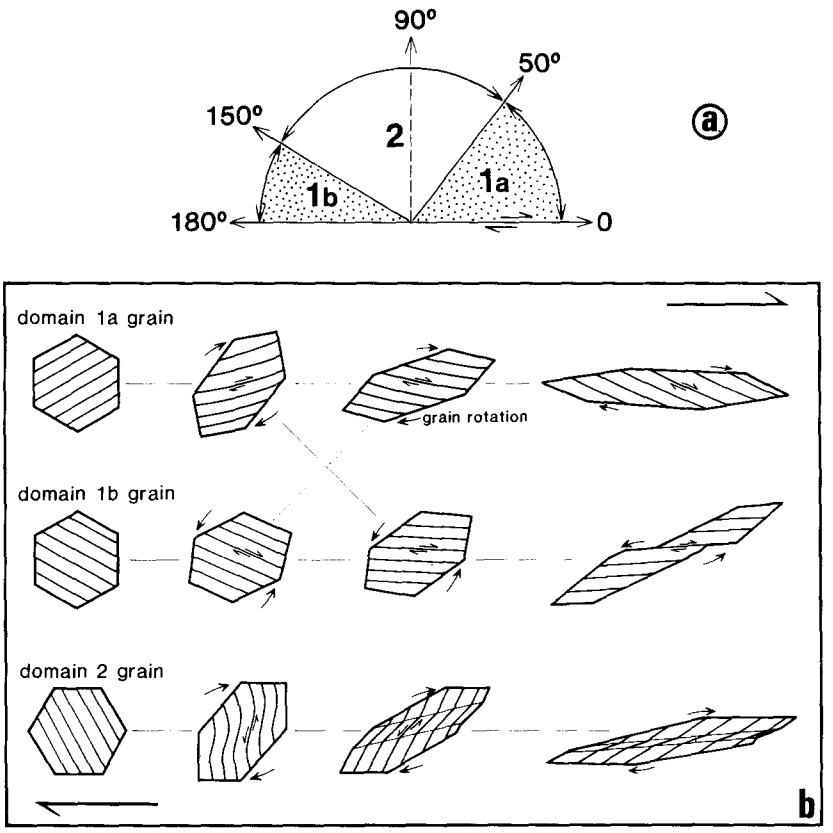

Fig. 11. The two-dimensional behaviour of grains and basal plane orientation in dextral shear (modified after Etchecopar 1977). It is assumed that the basal plane is orthogonal to the sketch plane. (a) The two orientation regimes that govern the sense of grain rotation. Domain 1, dotted area, corresponds to grains with (0001) oriented at low angles to the shear direction, domain 2 is a region where (0001) is at a high angle to the shear direction. (b) Behaviour of a grain with initial (0001) lying in different orientation ranges, and the deformation paths (solid lines) observed in these experiments. The broken lines represent other possible paths. Domain 1a (0–50°): at higher strains (0001) becomes bent to produce undulose extinction. However, grains with the final orientation are rarely observed and move into the 1b domain, but with a continued clockwise rotation. Domain 1b (150–180°): with large strains the deformation is heterogeneous and the grain separates into ribbon-like entities. Domain 2 (50–150°): deformation is inhomogeneous producing undulose grains, deformation bands and finally kink bands.

served. This growth cannot produce new orientations but it does decrease the percentage of grains in other orientations. In fact, grain-boundary migration appears to enhance the crystallographic preferred orientation by consuming grains oriented at a high angle to the shear direction as discussed above. These are the highly deformed augen and grains with the highest strain energy, and hence the least stable in the deforming aggregate. Conversely, grain growth preserves the elongate grains oriented with (0001) planes subparallel to the direction of easy glide.

Nucleation of equiaxed grains occurs at intragranular sites (Fig. 7) and dominantly in grains unsuitably oriented for glide. The new grain nucleation has the function of destroying, in part, any grain alignment produced during grain rotation. Subsequent grain growth preferentially occurs in a direction oblique to the shear direction (subparallel to the plane of flattening?) but is very irregular (e.g. irregular shaped grains in Fig. 6). The grain shape is controlled by the rate of boundary migration in a specific direction, that is before growth is arrested by impingement by other grains. Hence, the final shape depends on the pre-existing grain structure and the relative percentage of stable and highly oriented grains; that is, grains capable of undergoing further deformation by easy glide.

The deformation can be considered to be partitioned into two competing regions: (1) those where strain softening processes occur by dynamic recrystallization and (2) augen regions or hard spots that are undergoing little deformation and do not reflect the bulk shear strain. Hence, the contribution of the augen to the foliation will be offset while strain softening is occurring in the recrystallized areas. The 'foliation' will therefore no longer track the principal plane of finite strain and will not correspond with the theoretical flattening plane.

CONCLUSIONS

The role of dynamic recrystallization in coarser grained tectonites deformed at elevated temperatures and in a simple shear environment has received little attention. Extrapolation from analogue materials such as ice have important implications for geological envi-

ronments. The following important points emerge from these simple shear experiments on ice.

(1) It has been shown that dynamic recrystallization begins to occur at strains of the order of 2–3%. The various recrystallization processes can be conveniently divided into rotation and growth mechanisms. These are accompanied by the development of fabrics favouring glide on basal planes.

(2) Dynamic recrystallization is a strain softening process and locally partitions strain through the sample. There is abundant evidence to suggest that dynamic recrystallization contributes to the grain-shape changes in the sheared sample. It also prevents strain hardening and a change of deformation mechanisms to a regime of fracturing. Dynamic recrystallization is therefore an important part of the deformation process and hence can be considered to be a deformation mechanism as much as an accommodation mechanism.

(3) The measured shape fabric formed during simple shear does not correspond to the theoretical plane of flattening for the appropriate increment of shear strain. The preferred dimensional orientation defines a plane of anisotropy marked by a weak grain-shape fabric which also corresponds to a strong crystallographic orientation. Intracrystalline glide in individual grains becomes progressively easier as grains oriented for hard glide are rotated, deformed and dynamically recrystallized.

(4) Estimates of strain magnitude from grain shape and orientation are unreliable, beyond the fact that the more elongate grains have recorded higher local strains. The idea that grain shape and any corresponding foliation in a shear zone defined in part by deformed grains that were initially approximately equant, needs to be interpreted with caution. These experiments clearly show that this does not apply if there is continuous reworking of the grain structure by dynamic recrystallization.

(5) The rapid development of strong *c*-axis fabrics can be related to the reorientation of grains for easy slip and continued dynamic recrystallization. The preferred alignment of basal planes and their progressive rotation into parallelism with the shear direction favours a reduction in the flow stress by easy glide. This is a process of geometrical softening and in sheared ice this leads to a rapid increase in strain rate (Duval 1981). As the imposed shear strain increases there was no evidence for microfracturing or grain-boundary sliding. This experimental observation confirms the idea of White *et al.* (1980) that in higher temperature shear zones the deformation is predominantly by crystal plastic processes rather than involving superplastic phenomena.

Acknowledgements—The authors wish to thank the Australian Research Grants Committee for their financial sponsorship of the work described in this paper. The Glaciology section of the Australian Antarctic Division is thanked for the maintenance of the cold room facilities where experiments and specimen preparation were undertaken. J. P. Burg was supported by a University of Melbourne Research Fellowship. P. J. Hudleston and J-P. Poirier are thanked for their comments on the manuscript.

REFERENCES

Bouchez, J. L. & Duval, P. 1982. The fabric of polycrystalline ice deformed in simple shear: experiments in torsion, natural deformation and geometrical interpretation. *Text. Microstruc.* **5**, 171–190.

Burg, J. P., Iglesias, M., Laurent, Ph., Matte, Ph. & Ribeiro, A. 1981. Variscan intracontinental deformation: the Coimbra–Cordoba Shear Zone (SW Iberian Peninsula). *Tectonophysics* **78**, 161–177.

Chakrabarti, A. K. & Spretnak, J. W. 1975. Instability of plastic flow in the direction of pure shear. *Met. Trans.* **6A**, 733–747.

Cobbold, P. R. 1977. Description and origin of banded deformation structures—I. Regional strain, local perturbations, and deformation bands. *Can. J. Earth Sci.* **14**, 1721–1731.

Coward, M. P. 1976. Strain within ductile shear-zones. *Tectonophysics* **34**, 181–197.

Davis, G. H. 1983. Shear-zone model for the origin of metamorphic core complexes. *Geology* **11**, 342–347.

Duval, P. 1981. Creep and fabrics of polycrystalline ice under shear and compression. *J. Glaciol.* **27**, 129–140.

Escher, A., Escher, J. C. & Watterson, J. 1975. The reorientation of the Kangamuit dyke swarm, West Greenland. *Can. J. Earth Sci.* **12**, 158–173.

Etchecopar, A. 1977. A plane kinematic model of progressive deformation in a polycrystalline aggregate. *Tectonophysics* **39**, 121–139.

Hudleston, P. J. 1980. The progressive development of inhomogeneous shear and crystallographic fabric in glacial ice. *J. Struct. Geol.* **2**, 189–196.

Hutchinson, J. W. & Tvergaard, V. 1981. Shear band formation in plane strain. *Int. J. Solids Struct.* **17**, 451–470.

Jacka, T. H. 1984. Laboratory studies on relationships between ice crystal size and flow rate. *Cold Regions Sci. Technol.* **10**, 31–42.

Jonas, J. J., Holt, R. A. & Coleman, C. E. 1976. Plastic stability in tension and compression. *Acta metall.* **24**, 411–418.

Kamb, W. B. 1972. Experimental recrystallization of ice under stress. In: *Flow and Fracture of Rocks* (edited by Heard, H. C., Borg, I. Y., Carter, N. L. & Raleigh, C. B. *Mon. Am. geophys. Un.* **16**, 211–241.

Kuon, L. G. & Jonas, J. J. 1973. Effect of strain rate and temperature on the microstructure of polycrystalline ice. In: *Physics and Chemistry of Ice* (edited by Whalley, E., Jones, S. J. & Gold, L. W.). Royal Society Canada, Ottawa, 370–376.

Langway, C. C., Jr. 1958. Ice fabrics and the universal stage. U.S. Snow, Ice and Permafrost Research Establishment, Technical Report 62.

Lisle, R. J. 1977. Estimation of tectonic strain ratio from the mean shape of deformed elliptical markers. *Geol. Mijnb.* **56**, 140–144.

Lister, G. S. & Price, G. P. 1978. Fabric development in a quartz–feldspar mylonite. *Tectonophysics* **49**, 37–78.

Mandl, G., de Jong, L. N. J. & Maltha, A. 1977. Shear zones in granular material. *Rock Mechanics* **9**, 95–144.

Means, W. D. 1981. The concept of steady-state foliation. *Tectonophysics* **78**, 179–199.

Nicolas, A., Bouchez, J. L., Blaise, J. & Poirier, J. P. 1977. Geological aspects of deformation in continental shear zones. *Tectonophysics* **42**, 55–73.

Ohtomo, M. & Wakahama, G. 1982. Crystallographic orientation of recrystallized grain in strained single crystal of ice. *Low Temperature Sci.* **41A**, 1–11.

Poirier, J. P. 1976. *Plasticité à Haute Température des Solides Cristallins*. Eyrolles, Paris.

Poirier, J. P. 1980. Shear localization and shear instability in materials in the ductile field. *J. Struct. Geol.* **2**, 135–142.

Poirier, J. P. & Guillopé, M. 1979. Deformation induced recrystallization of minerals. *Bull. Soc. Fr. Minéral. Cristallogr.* **102**, 67–74.

Ramsay, J. G. & Graham, R. H. 1970. Strain variation in shear belts. *Can. J. Earth Sci.* **7**, 786–813.

Rudnicki, J. W. & Rice, J. R. 1975. Conditions for the localisation of deformation in pressure-sensitive dilatant materials. *J. Mech. Phys. Solids* **23**, 371–394.

Russell-Head, D. S. & Budd, W. F. 1979. Ice-sheet flow properties derived from bore-hole shear measurements combined with ice-core studies. *J. Glaciol.* **24**, 117–130.

White, S. H., Burrows, S. E., Carreras, J., Shaw, N. D. & Humphreys, F. J. 1980. On mylonites in ductile shear zones. *J. Struct. Geol.* **2**, 175–187.

Wilson, C. J. L. 1979. Boundary structures and grain shape in deformed multilayered polycrystalline ice. *Tectonophysics* **57**, T19–T25.

Wilson, C. J. L. 1986. Deformation induced recrystallization of ice:

the application of in-situ experiments. In: *Mineral and Rock Deformation Laboratory Studies* (edited by Hobbs, B. E. and Heard, H. C.). *Mon. Am. geophys. Un.* **36**, 213–232.

Wilson, C. J. L. & Russell-Head, D. S. 1982. Steady state preferred orientation of ice deformed in plane strain at −1°C. *J. Glaciol.* **28**, 145–160.

Wilson, C. J. L., Burg, J. P. & Mitchell, J. C. 1986. The origin of kinks in polycrystalline ice. *Tectonophysics* **127**, 27–48.